Available online at www.sciencedirect.com
ScienceDirect
Ceramics International 37 (2011) 2669–2677
CERAMICS INTERNATIONAL
www.elsevier.com/locate/ceramint

Antimony doping effect on barium titanate structure and electrical properties

M.M. Vijatović Petrović [a,*], J.D. Bobić [a], T. Ramoška [b], J. Banys [b], B.D. Stojanović [a]

[a] Institute for Multidisciplinary Research, Belgrade University, Kneza Višeslava 1, 11000 Belgrade, Serbia
[b] Faculty of Physics, Vilnius University, Sauletekio al. 9, Vilnius, Lithuania

Received 20 January 2011; received in revised form 5 April 2011; accepted 8 April 2011
Available online 15 April 2011

Abstract

Nanopowders of pure and antimony doped barium titanate ($BaTiO_3$-BT) were synthesized by polymeric precursors method based on Pechini process. Obtained powders were pressed and sintered at 1300 °C for 8 h. XRD analysis showed the formation of cubic crystal structure in all nanopowders and tetragonal in BT ceramics. The influence of antimony concentration on structure change, grain size reduction and microstructure development was analyzed. Dielectric behavior of pure and antimony doped ceramics was studied as a function of temperature and frequency. The significant dielectric properties modification as a consequence of doping with different antimony concentration was noticed. The electrical resistivity measurements pointed out that antimony concentration influenced also on materials change from insulator to semiconductor.

Keywords: A. Powders: chemical preparation; Sintering; B. Grain size; C. Electrical properties

1. Introduction

Intensive material science development has the great influence on a rapid increase in the number of advanced materials in the field of microelectronics. Special place in the group of electroceramic materials is given to materials based on barium titanate.

Barium titanate is ferroelectric material with perovskite structure which has been of practical importance for over 60 years due to its specific electrical properties. It great significance is based on possibility of wide application as ceramic capacitors, PTCR thermistors, piezoelectric sensors, optoelectronic devices, transducers, actuators etc. A large number of theoretic and experimental research have been used to study different synthesis and processing methods that could lead to obtaining new materials for various application in electronics. Some of those applications are connected with possibility of changing barium titanate insulating properties to semiconducting by adding different kind of dopants [1–3].

It is well known that incorporation of dopant ions on Ba or Ti place in the $BaTiO_3$ lattice leads to structural and microstructural changing as well as to electrical properties modification [4,5]. Sb^{3+} (0.90 Å) is exclusively incorporated at the Ba^{2+} (1.35 Å) site, while it cannot substitute Ti^{4+} (0.68 Å) due to its higher ion radius. Adding of Sb^{3+} as donor dopant at relatively low concentration initiates the formation of room temperature n-type semiconducting ceramics, whereas higher dopant concentration leads to insulating materials [6]. Even though usually added dopant amount is rather low, BT properties modification are quite obvious. To obtain required electrical properties the special attention has to be given to correlation between synthesis method and all processing parameters, obtained structure and final materials properties [7,8].

Thus, in this work the influence of antimony as a donor dopant on properties of barium titanate powders and ceramics prepared by polymeric precursors method was studied. Structure formation and microstructure development was monitored and its influence on electrical properties modification was investigated.

2. Experimental procedure

The polymeric precursor method (PPM) is chemical synthesis method, where the solutions of ethylene glycol, citric acid and metal ions are polymerized to a form of polyester-type resin. The metal ions can be immobilized in a

* Corresponding author. Tel.: +381 11 2085039; fax: +381 11 2085062.
E-mail address: miravijat@yahoo.com (M.M.V. Petrović).

0272-8842/$36.00
doi:10.1016/j.ceramint.2011.04.015

rigid polyester network, and no segregation of cations can be observed during thermal decomposition of the organic material [3].

The barium titanate powders for this investigation were prepared by polymeric precursors method, modified Pechini process. For preparing titanium citrate and barium citrate solutions as a starting materials titanium tetra-isopropoxide ($Ti[OCH(CH_3)_2]_4$, Alfa Aesar, 99.995%) and barium acetate ($Ba(CH_3COO)_2$, Alfa Aesar, 99.0–102.0%) were used. Ethylene glycol and citrate acid were used as solvents in both citrate solutions, where the molar ratio between metal ion, citric acid and ethylene glycol was 1:4:16. Barium citrate and titanium citrate solutions were mixed and heated at 90 °C. At this synthesis stage, antimony as a doping agent was added in the form of antimony acetate salt ($Sb(CH_3COO)_3$, Aldrich, 99.99%) with 0.1, 0.3 and 0.5 mol% Sb (BTS1, BTS3 and BTS5). Temperature was raised up to 120–140 °C, when transparent yellow solution changed to a solidified dark-brown glassy resin. The decomposition of the most organic part was performed in the oven at 200 °C for 4 h, with constant stirring and heating rate of 2 °C/min. As soon as the resin incinerated, and became black solid mass, material was pulverized. Thermal treatment was performed at temperatures ranging from 350 to 800 °C and each step lasted for 4 h. Detailed procedure could be found elsewhere [9]. The agglomerates were smashed by milling in agate pulverizer (Fritisch Pulverisette, Type 02.102). After drying at room temperature and sieving, the barium titanate powders were obtained [10–13].

BT powders were pressed into pellets under the pressure of 196 MPa using uniaxial press. Sintering was performed at 1300 °C for 8 h (in tube furnace Lenton, UK) in air atmosphere and the heating rate was 10 °C/min.

Particle size distributions (PSDs) were measured using laser diffraction (Malvern Mastersizer S) and specific surface areas (SSA) were obtained by nitrogen adsorption (Gemini 2375, Micromeritics). The average particle diameters (D_{BET}) were calculated from the SSA ($6/(\rho_{theoretical} \times SSA)$). Density of pure and doped barium titanate powders were measured using a He Pycnometer (Micromeritics AccuPyc 1330) and density of barium titanate ceramics was obtained by measuring dimensions and mass of the samples and calculating from equation $\rho = 4m/d^2h\pi$ (where m is mass, d – average diameter and h – height of the sintered samples). The microstructure and morphology of nanopowders and sintered samples were investigated using X-ray diffraction (Model Phillips PW1710 diffractometer) and scanning electron microscope (JEOL JSM-6610LV for powders and Tescan VEGA TS 5130MM for ceramic samples). The microstructures of sintered samples were observed at free and fracture surface and samples were coated with gold. The electrical measurements were carried out using an LCR meter (model 4284 A, Hewllet-Packard) and samples were prepared by applying Ag electrodes on the polished surfaces of the sintered ceramic disks. Since, from the electrical measurements were obtained values for real (ε') and imaginary (ε'') parts of permittivity, the dielectric loss tangent of barium titanate ceramics was derived calculating from equation $\tan\delta = \varepsilon''/\varepsilon'$. The total ac resistivities at room temperature were extracted from complex impedance spectrum (Nyquist plots) obtained from the variation of imaginary Z'' ($Z'' = \varepsilon'/2\pi f\varepsilon_0(\varepsilon''^2 + \varepsilon'^2)$) and real part, Z' ($Z' = \varepsilon''/2\pi f\varepsilon_0(\varepsilon'^2 + \varepsilon''^2)$) of impedance calculating form obtained permittivity data.

3. Results and discussion

The XRD analysis of all powders indicated the formation of cubic BT phase (identified using the JCPDS files no. 31-0174). Fig. 1 shows the XRD results of doped BT and it was not observed the difference between BTS1, BTS3 and BTS5 samples due to very small amount of added antimony which was less than sensitivity of used XRD equipment. The crystallite size of about 17 nm was obtained in all doped samples (calculated using Scherer's equation) and it was smaller in comparison with crystallites of pure BT powders (Table 1). This difference in crystallite size could be assigned to the substitution of larger barium with smaller antimony ion which influenced on appearance of crystal imperfections that could cause broadening of diffraction peaks [14–16].

The analysis of results obtained by particle size distribution could point out that obtained powders are nanosized with evident agglomeration. Densities of all doped powders were slightly higher than obtained for pure BT powder, 95.5 ± 0.1% of theoretic density. Specific surface area measurements of doped samples showed higher values in comparison with pure BT powders. Therefore, calculated average particle size, D_{BET}, was smaller, with particles 58 ± 1 nm. These results indicate that synthesized powders were nanosized and point that antimony as a donor dopant has influence on BT particle size reduction (Table 1) [17].

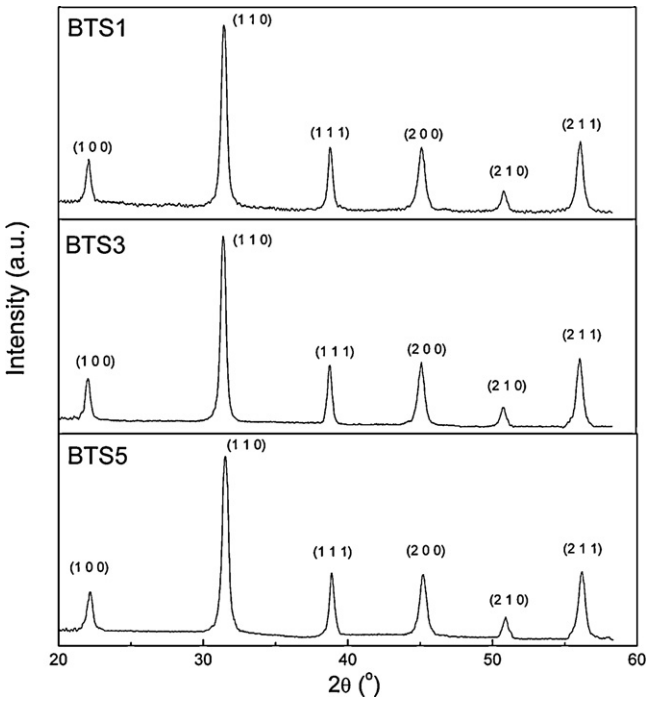

Fig. 1. XRD results of (a) BTS1, (b) BTS3 and (c) BTS5 powders.

Table 1
Results obtained for pure and doped barium titanate powders.

Sample	D_{XRD} (nm)	D_{V50} (nm)	SSA (m^2/g)	D_{BET} (nm)	D_{SEM} (nm)
BT	20–23	6530	13.47	74.07	40
BTS1	16–17	9321	16.99	58.68	∼35
BTS3	17–18	8790	16.94	58.87	∼35
BTS5	16–17	8320	17.48	57.04	∼35

Fig. 2 shows the SEM micrographs of the BT powders. The primary particles in all powders have rounded shape with size ∼40 nm for pure and ∼35 nm for doped samples with presence of agglomerates.

It is well known that nanostructured ceramics is very hard to obtain due to a lot of factors that could affect the process of ceramics producing and its final properties. Thus, the degree of powder agglomeration, sintering regime (temperature, time and atmosphere) and dopants can have high effect on densification and BT microstructure [18,19].

The XRD results (Fig. 3) of sintered samples show formation of barium titanate tetragonal crystal structure which is identified by appearance of its characteristic diffraction peaks (JCPDS files no. 05-0626). Calculated lattice parameters confirmed the formation of tetragonal structure in all samples. The tetragonality found in doped samples BTS1 and BTS3 was higher than for pure BT sample obtained by PPM (Table 2). In doped samples tetragonality decreased with increasing of

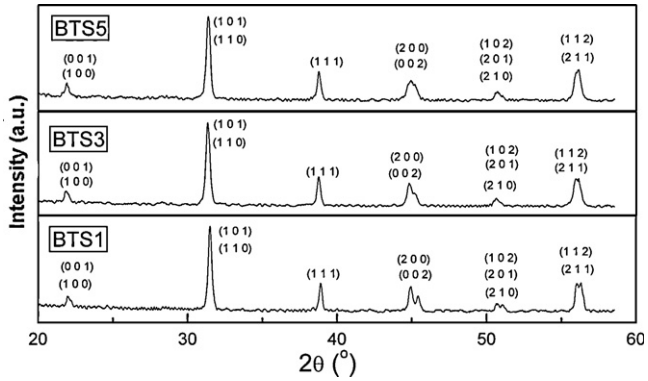

Fig. 3. XRD diffractograms of BTS1, BTS3 and BTS5 samples sintered at 1300 °C/8 h.

dopant concentration indicating the structure change from tetragonal to pseudo-cubic. The ratio *c/a* for pure BT was 1.0053 and it is in agreement with values for BT obtained by other chemical synthesis methods published by other authors [5,20].

The splitting of some diffraction peaks can be seen in Fig. 3 and that is especially prominent for $2\theta = 45^{\circ}$. The appearance of new reflections or their splitting at XRD diagrams indicates changing of symmetry in BT perovskite structure. Therefore, adding of dopants in the structure could lead to this symmetry change due to appearance of irregularities in ions packaging in BT lattice [21]. In the homogenous and fine grained materials, the emergence of mechanical stress also leads to stabilization of

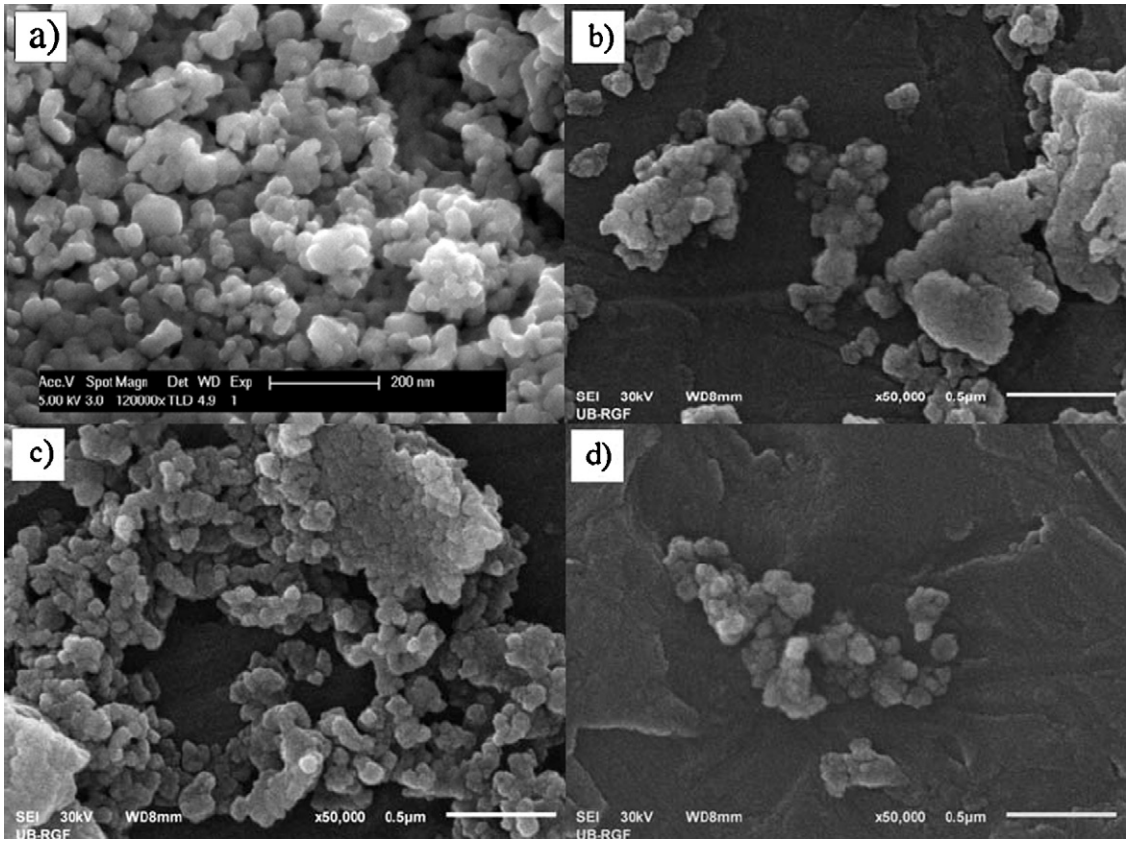

Fig. 2. SEM photographs of (a) BT, (b) BTS1, (c) BTS3 and (d) BTS5 barium titanate powders.

Table 2
Lattice parameters, tetragonality, average grain size and density value for different specimens of barium titanate ceramics.

Sample	*a*	*b*	*c*	*c/a*	D_{SEM} (μm)	Density (%)
BT	3.9968	3.9968	4.0180	1.0053	1.0–2.5	90.1
BTS1	3.9968	3.9968	4.0368	1.0100	0.8–1.0	88.5
BTS3	4.0100	4.0100	4.0404	1.0076	0.5	94.4
BTS5	4.0095	4.0095	4.0291	1.0049	0.45	96.7

pseudo-cubic structure [22,23]. Buscaglia et al. [5] assumed that XRD peaks symmetry lowering is connected with existing of two structurally different regions, cubic and tetragonal, within doped BT grains. They considered this phenomenon as a connection between dopant incorporation in the BT lattice and transition of material from ferroelectric to paraelectric phase in doped BT.

Wu et al. [24] studied tetragonality change in pure BT samples with different grain sizes. These authors concluded that the highest *c/a* ratio was found in samples with the biggest grains and this ratio becomes lower as the concentration of smaller grains in the sample increases. Therefore, this is in agreement with our study, where dopants were added in order to reduce grain size and as a result of grain lowering, the symmetry was changed and materials crystal structure was switched from tetragonal to pseudo-cubic.

Fig. 4 shows microstructures of barium titanate ceramics sintered at 1300 °C for 8 h. Microstructural analysis showed that grains were rounded or polygonal in shape but there were

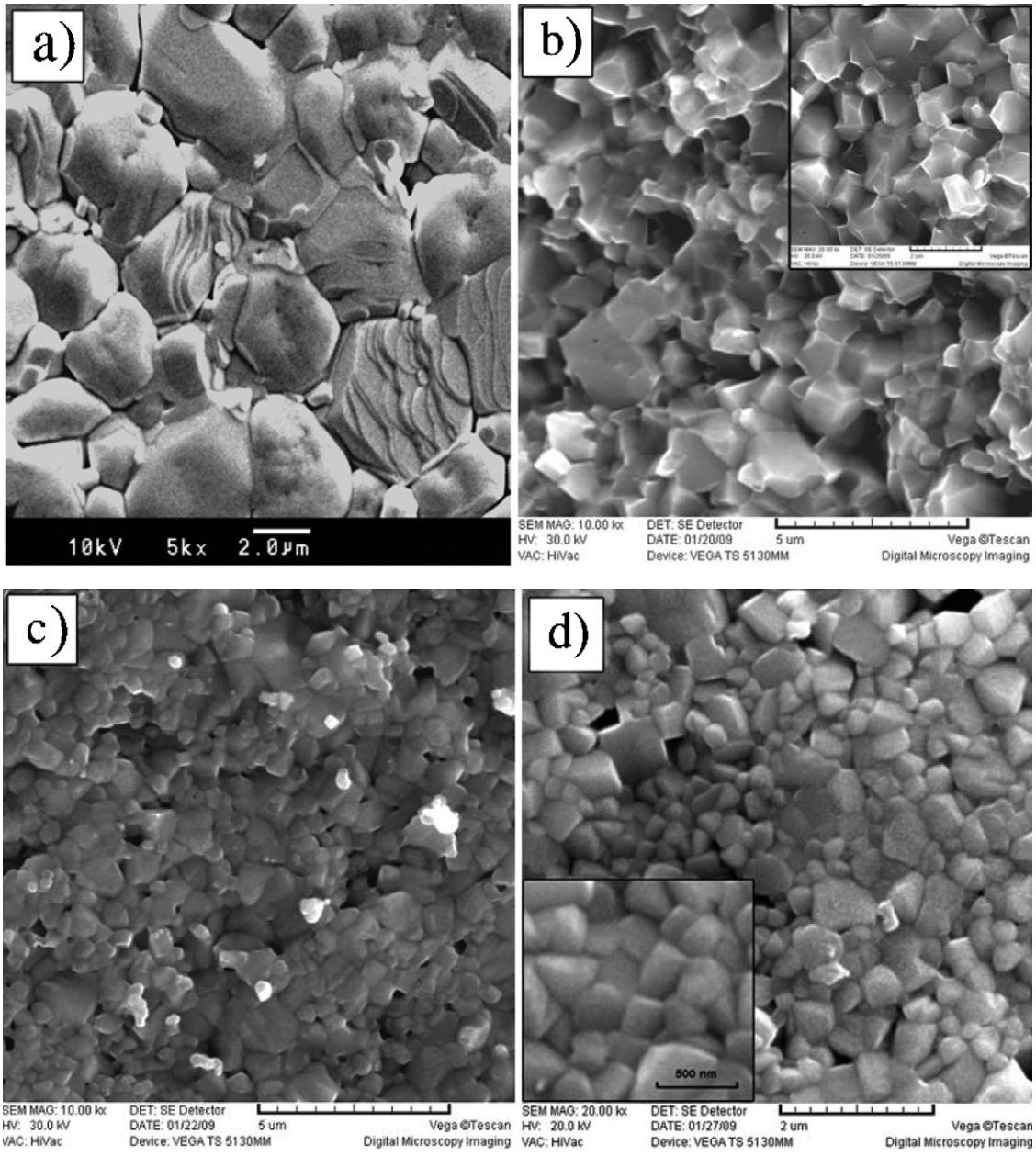

Fig. 4. Micrographs of barium titanate specimens sintered at 1300 °C for 8 h (a) BT, (b) BTS1, (c) BTS3 and (d) BTS5.

also differences in grain size, homogeneity and porosity between samples doped with different concentration of antimony (Table 2). Grains observed in doped samples were smaller in comparison with pure BT and as the concentration of antimony became higher the grains size was smaller. Even very low concentration of antimony could inhibit grain growth in BT ceramics significantly. Samples doped with 0.5 mol% of antimony have shown the largest grain size reduction to around 0.45 μm. In samples BTS5 and BTS3 the bimodal grain size distribution can be observed, where beside smaller grains, bigger grains with size ∼1 μm can be noticed, probably associated with non-uniform dopant distribution in the barium titanate.

The sample color was changed after sintering, from pale yellow for BTS1 sample, to light blue for BTS3 and dark blue for BTS5. This is an indication that material is turning into n-type semiconductor [25,26].

The dielectric properties of samples obtained by PPM and sintered at 1300 °C for 8 h were studied. The temperature dependence of dielectric constant was established in the temperature range −175 to 175 °C and the frequency range from 50 kHz to 1 MHz.

Fig. 5 represents temperature dependence of dielectric constant of BT ceramics. Dielectric anomalies that correspond to three structural transitions (cubic to tetragonal – $T_{C\text{-}T}$, tetragonal to orthorhombic – $T_{T\text{-}O}$, orthorhombic to rhombohedral – $T_{O\text{-}R}$) could be detected for pure BT and sample BTS1 on a curve typical for classical ferroelectric material. On the other hand, in samples doped with higher dopant concentration (BTS3 and BTS5) low temperature phase transitions cannot be clearly observed. It could be noticed that the shape of curves was changed as well as peaks positions. As the concentration of antimony increases, structural transitions that correspond to $T_{C\text{-}T}$ and $T_{T\text{-}O}$ were shifted to the lower temperatures, whereas $T_{O\text{-}R}$ was at the same position (Table 3). The rather broad peak was observed for $T_{T\text{-}O}$ transition and small but still visible and well defined peak for $T_{C\text{-}T}$ phase transition. As it was explained by Rivera et al. [27], the broad ferroelectric phase transition can

Table 3
Transition temperatures and dielectric constant values for all samples at 100 kHz.

Sample	$T_{C\text{-}T}$ (°C)	$T_{T\text{-}O}$ (°C)	$T_{O\text{-}R}$ (°C)	ε' (T_{room})	ε' (T_C)
BT	120	14	−74	805	1280
BTS1	120	14	−74	699	1010
BTS3	96	10	−74	10,796	11,227
BTS5	99	7	−74	7457	7507

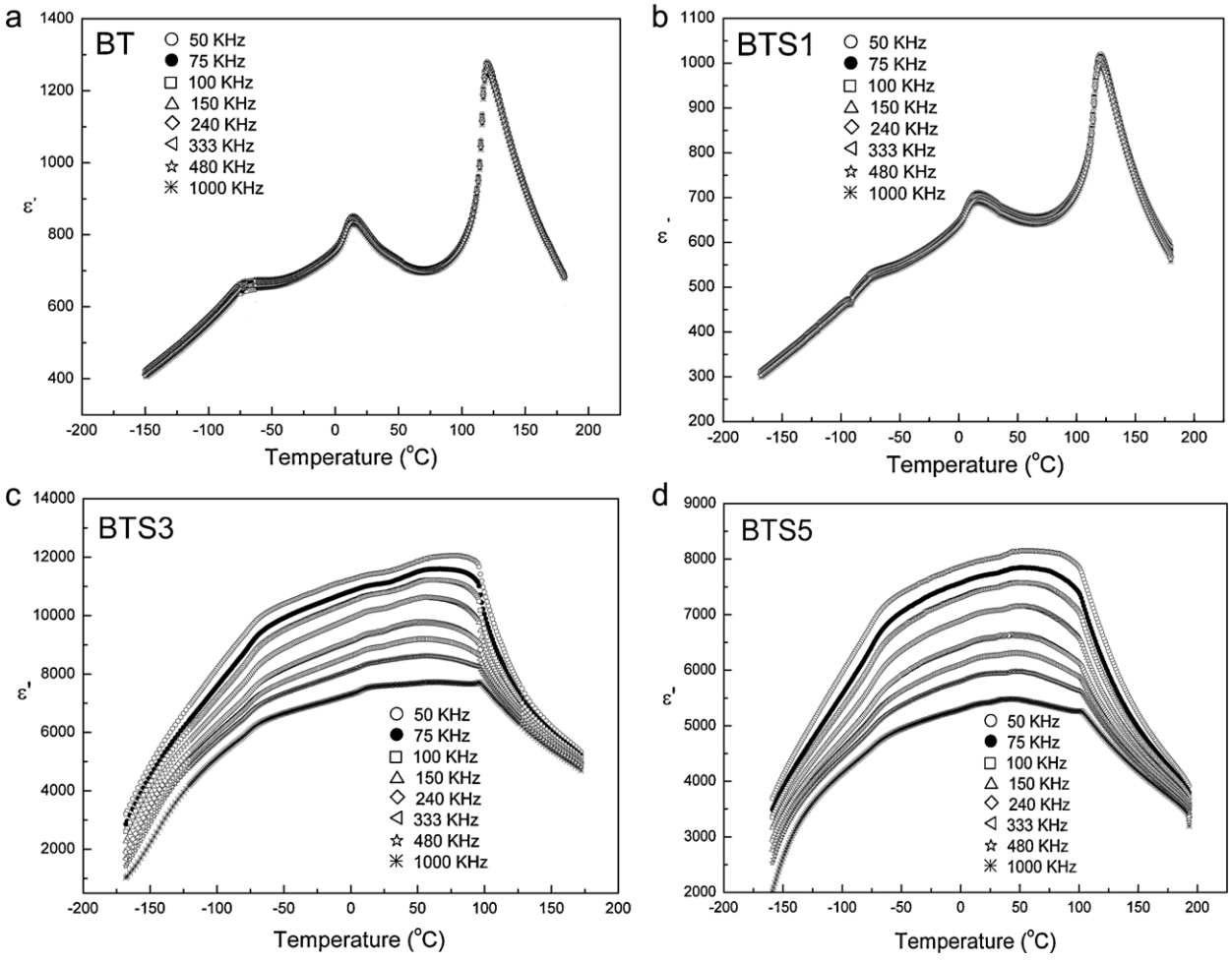

Fig. 5. Temperature dependence of dielectric constant in the frequency range from 50 kHz to 1 MHz for (a) BT, (b) BTS1, (c) BTS3 and (d) BTS5.

indicate the formation of diffuse ferroelectric. The appearance of small temperature dependence of dielectric constant in large range of T (from 0 to 100 °C) points to a thermal stability of ε for BTS3 and BTS5.

Some authors assumed that the reason for lowering of $T_{C\text{-}T}$ is smaller size of Sb^{3+} as compared to Ba^{2+} which makes tetragonal phase unstable or due to Ti vacancies formation which break Ti–O–Ti linkages, responsible for ferroelectricity in the material [28]. Other authors have connected this phenomenon with grains size decrease in doped samples, chemical composition and crystal imperfections [19,29–32].

The plots presented in Fig. 5 point out that addition of antimony leads to increase of dielectric constant value (Table 3). BTS1 ceramics possess slightly lower dielectric constant value than pure BT ceramics, so a small amount of antimony is not enough for significant dielectric properties modification. However, BTS3 ceramic has the highest dielectric constant and after addition of 0.5 mol% of antimony dielectric constant slightly decreases. Possible reason for dielectric constant increase could be the existence of small grains in doped samples and on the other hand, reaching the critical grain size could influence on further decrease of dielectric constant value [18,29,33,34]. Luan et al. [18] pointed out that decrease of grain size, even in pure BT, influences on ε increasing until it reaches ∼0.7–1 μm and further grain decrease leads to ε lowering. This study is in agreement with our results. Literature data [6,22] has shown that full incorporation of antimony in BT lattice is achieved by adding around 0.3 mol% of antimony where dopant is being distributed in grains that have dielectric properties. Therefore, adding of 0.5 mol% of antimony could cause its distribution in grains but also in grain boundaries which could affect on dielectric constant decrease [5]. The above observation indicates that the dopant concentration play the crucial role for dielectric properties modification.

Dielectric loss tangent as a function of temperature is shown in Fig. 6 the values of tan δ under 0.035 for pure and BTS1 were found. On the other hand, BTS3 and BTS5 have shown the highest values of tan δ (around 0.35). At high temperatures BT and BTS1 ceramics dielectric losses showed increase and frequency dispersion in paraelectric state (Fig. 6a and b) and it can be related to thermally activated Maxwell-Wagner relaxation [35]. In BTS3 and BTS5 dielectric losses decrease at high temperatures in all frequency range showing high frequency dispersion near the dielectric maximum.

The frequency dependence of dielectric constant at room temperature is shown in Fig. 7. The dielectric constant of all

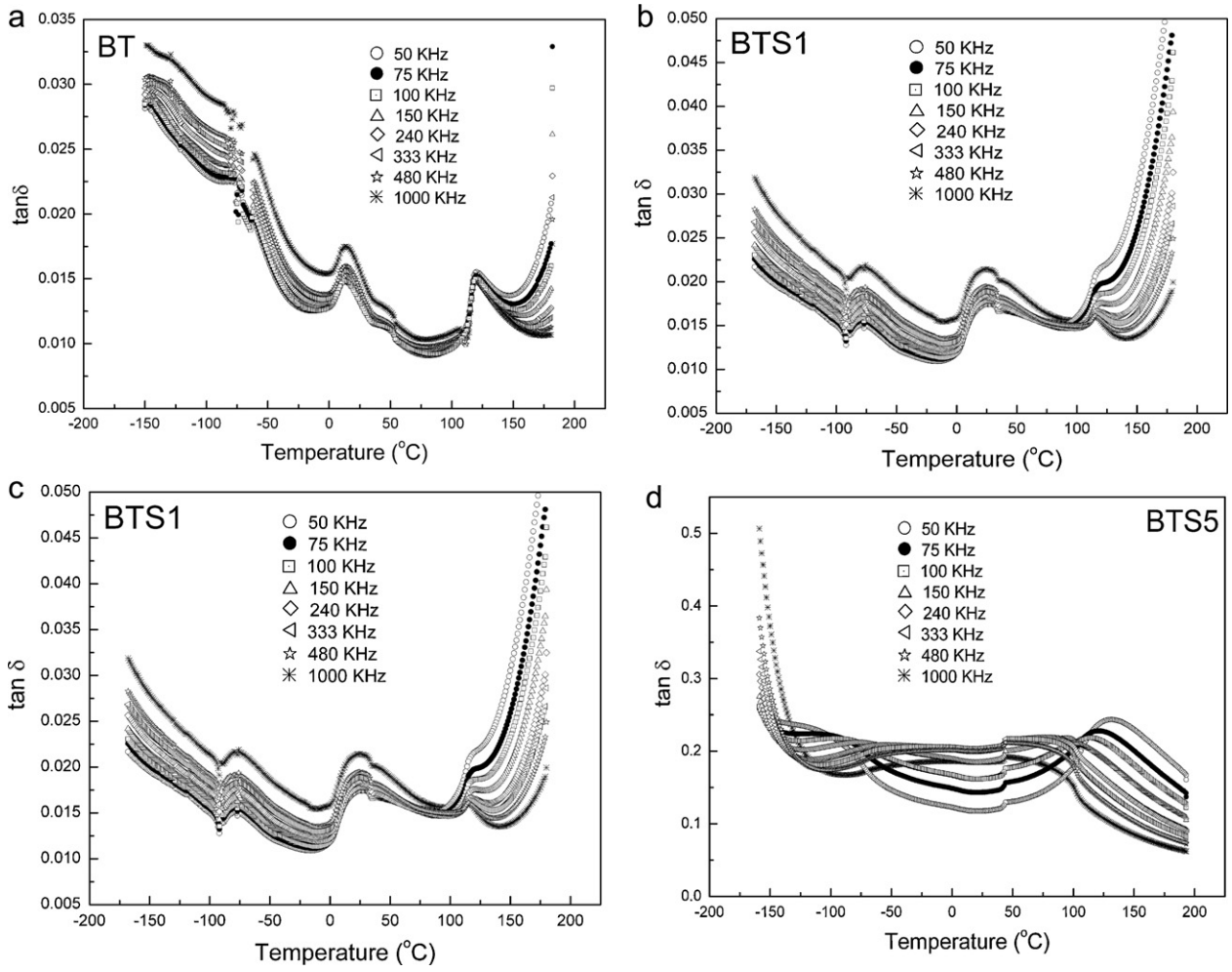

Fig. 6. Temperature dependence of dielectric losses in the frequency range from 50 kHz to 1 MHz for (a) BT, (b) BTS1, (c) BTS3 and (d) BTS5.

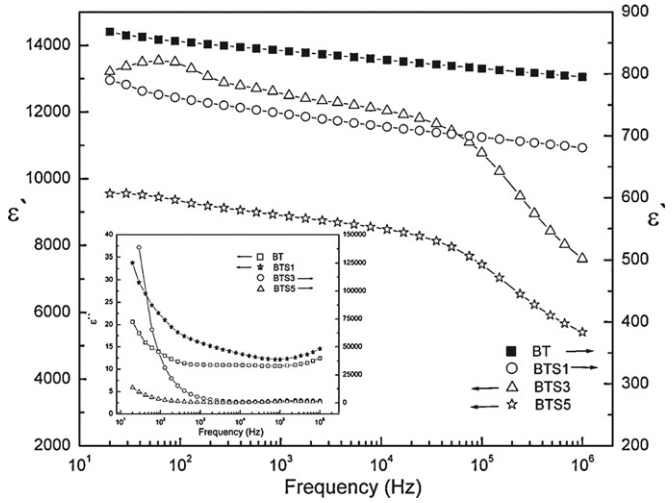

Fig. 7. Frequency dependence of real part of permittivity for pure and Sb doped BT samples at room temperature. Inset illustrates frequency dependence of imaginary part of permittivity for all BT ceramics.

samples decreased with increasing of frequency. In the case of BT and BTS1 samples, the decrease was almost linear in all frequency range. The dielectric constant of BTS3 has anomaly at around 60 Hz and further it decreased almost linearly until frequency reached 50 kHz and then it decreased rapidly. BTS5 sample followed the similar trend, although in this case there is no anomaly at low frequencies.

More detailed insight into relaxation of dielectric permittivity and dielectric loss have shown that in all compositions there is non-Debye behavior due to absence of typical broad Debye-like relaxation peak of $\varepsilon''(f)$ [36]. The increase of both, real and imaginary parts of permittivity can be observed at low frequencies, i.e. $f < 5 \times 10^2$ Hz (Fig. 7). In general, the tendency of ε'' to increase with frequency decrease indicates the onset of the Maxwell-Wagner effect [36]. Such a low frequency relaxation can have different origins and may be related to conductivity, to Maxwell-Wagner relaxation at grain boundaries and internal imperfections indicating that the origin of dielectric behavior of obtained BT ceramics is rather complex. Further, it is well known that many ceramic materials are electrically heterogeneous with semiconducting (or more conducting) grain cores separated by insulating (or less conducting) grain boundaries. The more insulating character of the grain boundaries can be associated with deviation from stoichiometry, segregation of impurities or formation of thin grain boundary secondary phase layer during the sintering process and grain boundary reoxidation during cooling [37]. Therefore, we assumed the possible accumulation of dopant at grain boundaries, indicating than this Maxwell-Wagner effect is due to small grain boundary electrical inhomogeneitis or because of the presence of oxygen or cation vacancies (Ti^{4+} and Ba^{2+}) in the sintered ceramics [35].

Dielectric loss tangent for all samples have shown frequency dependence as well (Fig. 8). Dielectric losses were quite low, under 0.03 for BT and BTS1 (Fig. 8a). Pure BT showed frequency independence in frequency range form 0.6 to

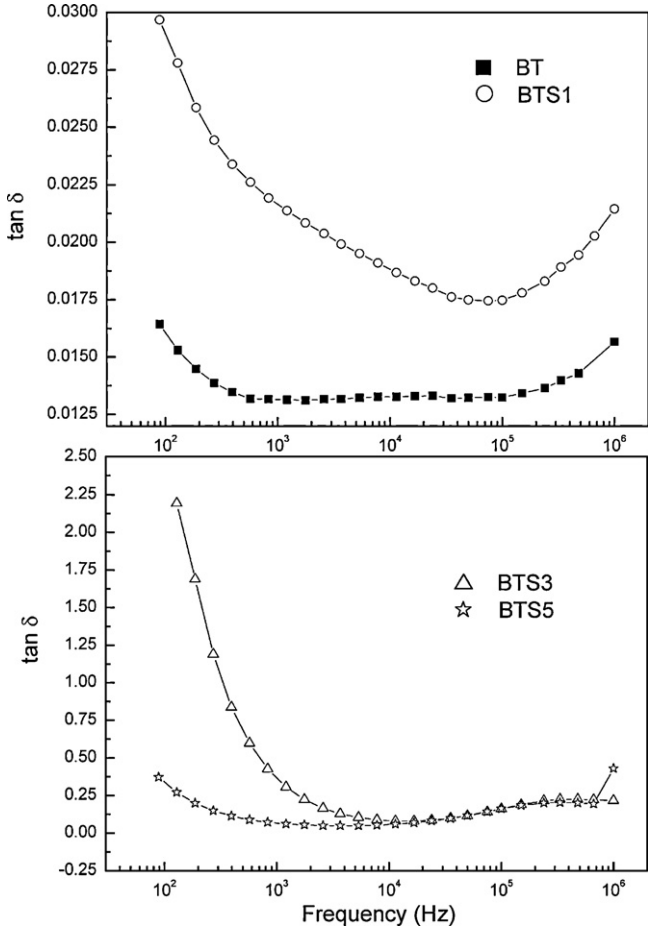

Fig. 8. Frequency dependence of dissipation factor for pure and Sb doped BT samples at room temperature.

100 kHz. Tan δ of BTS1 showed decrease till it reached value around 0.0175 at 70 kHz and then it increased. From Fig. 8b it could be noted that tangent loss of BTS3 decreases rapidly and goes through the minimum at 8 kHz ($\tan\delta = 0.08$) and then reaches the maximum around 300 kHz. Similar curve was found for BTS5 sample, where tan δ minimum of 0.0812 was observed in the range from 1 to 8 kHz and further maximum at 350 kHz. It was determined that for tan δ minimum, the dielectric constant was rather high, around 7500 for BTS5 and 11,000 for BTS3.

It was assumed that when added small amount of donor dopants in BT, the materials resistivity depends mainly on free carries concentration and its motion. Further increase of donor dopant concentration could cause the appearance of titanium and barium vacancies and materials resistivity rises again [6]. In our study, pure and barium titanate doped with 0.1 mol% Sb showed high electrical resistivity at room temperature (ac resistivity) $>10^8\ \Omega$ cm, that remark insulating behavior of these materials. However, for BTS3 and BTS5 materials resistivity was around 5.5×10^3 and $6.5 \times 10^4\ \Omega$ cm, respectively (Fig. 9). The lowest resistivity obtained for BTS3 was perhaps due to more uniform and complete incorporation of dopant in BT lattice and high concentration of free carriers. Nevertheless, the resistivity of BTS5 showed slight increase,

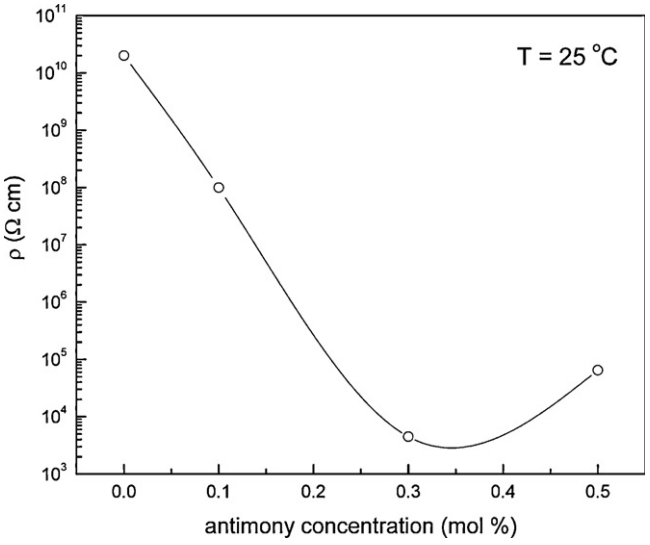

Fig. 9. Resistivity as a function of antimony concentration at room temperature.

suggesting also the possibility that dopant accumulated at grain boundaries increased the resistivity of material. In Fig. 9 is shown that room temperature resistivity minimum is around 0.35 mol% of added antimony. This concentration is possibly the critical value when free carries concentration decreases and vacancies appear in the material, influencing on resistivity change. More complete study about electrical resistivity and PTCR effect in BT doped materials will be subject of the future investigation.

4. Conclusion

Modified Pechini process was used for synthesis of pure and antimony doped barium titanate nanopowders. It was demonstrated that cubic nanopowders with particles from 40 to 35 nm were obtained. Tetragonality values obtained from XRD analysis proved the effect of antimony concentration on crystal structure, where structure was changed from tetragonal to pseudo-cubic. The influence of antimony content on BT microstructure was studied, indicating that antimony acts as a grain growth inhibitor and as its concentration increases grain size decreases. Microstructure changes that occur in doped BT led to dielectric properties modification. Antimony content in BT ceramics influenced on shifting of temperature phase transition peaks to the lower temperatures and broadening of ε–T curves. Dielectric constant value in doped BT was much higher than in pure BT ceramics, reaching values up to 11,227 for BT doped with 0.3 mol% Sb, whereas further addition of Sb led to its slight decrease. This appearance was assumed to be the result of different dopant incorporation in BT grains. It was also observed that dielectric constant and dielectric losses of pure and doped BT had shown certain frequency dependence and it was assumed the formation of diffuse ferroelectric material in BTS3 and BTS5. The influence of added dopant concentration on resistivity of obtained materials was also observed.

Generally, the addition of low concentration of antimony as a donor dopant could have the effect on BT crystal structure change, grain size reducing and furthermore on electrical properties modification.

Acknowledgements

The authors gratefully acknowledge the Ministry of Science and Technological Development Republic of Serbia for the financial support of this work (projects III45021) and COST 539.

References

[1] F. Jona, G. Shirane, Ferroelectric Crystals, Dover Publications Inc, New York, 1993.
[2] A.J. Moulson, J.M. Herbert, Electroceramics, second Ed., John Wiley & Sons Ltd, England, 2003.
[3] P. Kumar, S. Singh, M. Spah, J.K. Juneja, C. Prekash, K.K. Raina, Synthesis and dielectric properties of substituted barium titanate ceramics, J. Alloys Compd. 489 (2010) 59–63.
[4] M.T. Buscaglia, V. Buscaglia, M. Viviani, Atomistic simulation of dopant incorporation in barium titanate, J. Am. Ceram. Soc. 84 (2) (2001) 376–384.
[5] M.T. Buscaglia, V. Buscaglia, M. Viviani, P. Nanni, M. Hanuskova, Influence of foreign ions on the crystal structure of $BaTiO_3$, J. Eur. Ceram. Soc. 20 (2000) 1997–2007.
[6] E. Brzozowski, A.C. Caballero, M. Villegas, M.S. Castro, J.F. Fernandez, Effect of doping method on microstructural and defect profile of Sb–$BaTiO_3$, J. Eur. Ceram. Soc. 26 (2006) 2327–2336.
[7] M.M. Vijatović, J.D. Bobić, B.D. Stojanović, History and challenges of barium titanate: Part II, Sci. Sinter. 40 (2008) 235–244.
[8] M.M. Ristić, Principles of Materials Science, Scientific book, Belgrade, 1977.
[9] M.M. Vijatović, B.D. Stojanović, J.D. Bobić, T. Ramoška, P. Bowen, Properties of lanthanum doped $BaTiO_3$ produced from nanopowders, Ceram. Int. 36 (2010) 1817–1824.
[10] M.P. Pechini, N. Adams, United States Pattent No 3, 330, 697, 1967.
[11] M. Kakihana, M. Arima, Y. Nakamura, M. Yashima, M. Yoshimura, Spectroscopic characterization of precursors used in the Pechini-type polymerizable complex. Processing of barium titanate, Chem. Mater. 11 (1999) 438–450.
[12] L. Ramajo, R. Parra, M. Reboredo, M. Zaghete, M. Castro, Heating rate and temperature effects on the $BaTiO_3$ formation by thermal decomposition of (Ba,Ti) organic precursors during the Pechini process, Mater. Chem. Phys. 107 (2008) 110–114.
[13] W.S. Cho, E. Hamada, Synthesis of ultrafine $BaTiO_3$ particles from polymeric precursors: their structure and surface property, J. Alloys Compd. 266 (1998) 118–122.
[14] S. Kasap, P. Capper, Springer Handbook of Electronic and Photonic Materials, Springer Science+Business Media Inc, New York, 2006.
[15] A. Koelzynski, K. Tkacz-Smiech, From the molecular picture to the band structure of cubic and tetragonal barium titanate, Ferroelectrics 314 (2005) 123–134.
[16] R.C. Buchanan, Ceramic Materials for Electronics, Marcel Dekker Inc, New York, 1986.
[17] S. Tangjuanak, T. Tunkasiri, Characterization and properties of Sb-doped $BaTiO_3$ powders, Appl. Phys. Lett. 90 (2007) 072908.
[18] W. Luan, L. Gao, J. Guo, Size effect on dielectric properties of fine-grained $BaTiO_3$ ceramics, Ceram. Int. 25 (1999) 727–729.
[19] B.D. Stojanovic, M.A. Zaghete, C.R. Foschini, F.O.S. Vieira, J.A. Varela, Structure and properties of donor doped barium titanate prepared by citrate process, Ferroelectrics 270 (2002) 15–20.
[20] T.C. Huang, M.T. Wang, H.S. Sheu, W.F. Hsieh, Size-dependant lattice dynamics of barium titanate nanoparticles, J. Phys. Condens. Matter. 19 (2007) 476212 (12 pp).
[21] Lj. Karanovic, Applied Crystallography, University of Belgrade, Belgrade, 1996.

[22] E. Brzozowski, M.S. Castro, Influence of Nb^{5+} and Sb^{3+} dopants on the defect profile, PTCR effect and GBBL characteristics of $BaTiO_3$ ceramics, J. Eur. Ceram. Soc. 24 (2004) 2499–2507.
[23] Z.Z. Lazarevic, M.M. Vijatovic, B.D. Stojanovic, M.J. Romcevic, N.Z. Romcevic, Structure study of nanosized La- and Sb-doped $BaTiO_3$, J. Alloys Compd. 494 (2010) 472–475.
[24] L. Wu, M.C. Chure, K.K. Wu, W.C. Chang, M.J. Yang, W.K. Liu, M.J. Wu, Dielectric properties of barium titanate ceramics with different materials powder size, Ceram. Int. 35 (2009) 957–960.
[25] M.E.V. Costa, P.Q. Mantas, Dielectric properties of porous $Ba_{0.997}La_{0.003}Ti_{1.0045}O_3$ ceramics, J. Eur. Ceram. Soc. 19 (1999) 1077–1108.
[26] A.F. Shimanskij, M. Drofenik, D. Kolar, Subsolidus grain growth in donor doped barium titanate, J. Mater. Sci. 29 (1994) 6301–6305.
[27] I. Rivera, A. Kumar, N. Ortega, R.S. Katiyar, S. Lushnikov, Devide line between relaxor, diffused ferroelectric, ferroelectric and dielectric, Solid State Commun. 149 (2009), 172-146.
[28] F.D Morrison, D.C. Sinclair, A.R. West, Electrical and structural characteristics of lanthanum-doped barium titanate ceramics, J. Appl. Phys. 86 (1999) 6355–6366.
[29] G. Arlt, D. Hennings, G. de With, Dielectric properties of fine-grained barium titanate ceramics, J. Appl. Phys. 58 (4) (1985) 1619–1625.
[30] S. Chatterjee, B.D. Stojanovic, H.S. Maiti, Effect of additives and powder preparation techniques on PTCR properties of barium titanate, Mater. Chem. Phys. 78 (2003) 702–710.
[31] S.M. Bobade, D.D. Gulwade, A.R. Kulkarni, P. Gopalan, Dielectric properties of A- and B-site doped $BaTiO_3$ (I): La- and Al-doped solid solution, J. Appl. Phys. 97 (2005) 074105.
[32] M. Kuwabara, H. Matsuda, N. Kurata, E. Matsuyama, Shift of the curie point of barium titanate ceramics with sintering temperature, J. Am. Ceram. Soc. 80 (1997) 2590–2596.
[33] M.T. Buscaglia, V. Buscaglia, M. Viviani, J. Petzelt, M. Savinov, L. Mitoseriu, A. Testino, P. nanni, C. Harnagea, Z. Zhao, M. Nygren, Ferroelectric properties of dense nanocrystalline $BaTiO_3$ ceramics, Nanotechnology 15 (2004) 1113–1117.
[34] O.P. Thakur, C. Prakash, A.R. James, Enhanced dielectric properties in modified barium titanate ceramics through improved processing, J. Alloys Compd. 470 (2009) 548–551.
[35] N. Horchidan, A. Ianculescu, L. Curecheriu, F. Tudorache, V. Musteata, S. Stoleriu, N. Dragan, D. Grisan, S. Tascu, L. Mitoseriu, Preparation and characterization of barium titanate stannate solid solutions, J. Alloys Compd. 509 (2011) 4731–4737.
[36] D. O'Neill, R.M. Bowman, J.M. Gregg, Dielectric enhancement and Maxwell-Wagner effects in ferroelectric superlattice structure, Appl. Phys. Lett. 77 (2000) 1520–1522.
[37] M. Viviani, M. Bassoli, V. Buscaglia, M.T. Buscaglia, P. Nanni, Giant permittivity and Maxwell-Wagner relaxation in Yb:$CaTiO_3$ ceramics, J. Phys. D 42 (2009) 175407.